

COMPLEXATION OF SOME ALKALINE EARTH METALS WITH BIDENTATE URACIL LIGAND: SYNTHESIS, SPECTROSCOPIC AND ANTIMICROBIAL ANALYSIS

Ayman A.O. Younes¹, Moamen S. Refat^{2*}, Hosam A. Saad², Abdel Majid A. Adam², Omar M. Alzoghbi³, Ghayah M. Alsulaim⁴ and Amnah Mohammed Alsuhaibani⁵

¹Department of Chemistry, Faculty of Science, University of Bisha, Bisha 61922, Saudi Arabia

²Department of Chemistry, College of Science, Taif University, P.O. Box 11099, Taif 21944, Saudi Arabia

³Department of Chemistry, College of Science and Art, Imam Mohammad Ibn Saud Islamic University (IMSIU), Huraymla 15433, Saudi Arabia

⁴Chemistry department, faculty of Science, the Eastern Province, Al-Ahsa-King Faisal University, Saudi Arabia.

⁵Department of Physical Sport Science, College of Education, Princess Nourah bint Abdulrahman University, P.O. Box 84428, Riyadh 11671, Saudi Arabia

(Received January 24, 2022; Revised March 8, 2023; Accepted March 10, 2023)

ABSTRACT. Magnesium, calcium, strontium, and barium complexes of uracil were prepared in a 2:1 ligand to metal ratio to investigate the ligational character of the uracil (Ura). The modes of chelation were explained depending on elemental analyses, FT. IR, ¹H-NMR spectra as well as scanning electron microscopy. Uracil has two donation sites either through N₍₃₎ and C₍₂₎=O, or through N₍₃₎ and C₍₄₎=O with the molecular formulas [M(Ura)₂(H₂O)₂]Cl₂ where M = Mg(II), Ca(II), Sr(II) and Ba(II). The morphological surface and particle size of uracil metal complexes were determined using SEM and TEM. The thermal behaviors of the complexes were studied by the TGA (DTG) technique. The data obtained agreed well the proposed structures and showed that the complexes were finally decomposed to the corresponding metal oxide. The thermodynamic parameters are calculated from the thermal analysis curves using the Coats-Redfern and Horowitz-Metzger methods. The negative values of ΔS[‡] deduced the ordered structures of the prepared complexes compared to their starting reactants. Antibacterial activity of ligands and complexes is evaluated with two types of bacteria *Staphylococcus aureus* (gram-positive) and *Escherichia coli* (gram-negative) by the agar-well diffusion technique using DMSO as a solvent.

KEY WORDS: Uracil, Coordination compounds, Non-isothermal kinetic parameters, Elemental analysis, Spectral studies, Biological efficiency

INTRODUCTION

Uracil (C₄H₄N₂O₂) is a naturally occurring pyrimidine derivative and one of the four nucleobases in RNA in which uracil binds to adenine *via* two hydrogen bonds. 2,4(1H, 3H)-Pyrimidinedione commonly called through the trivial name uracil. Other names of (Ura) is 2-oxy-4-oxy pyrimidine or 2,4-dihydroxy pyrimidine or 2,4 pyrimidine diol [1]. Uracil exists in two tautomeric forms as given in Figure 1, amide tautomer called lactam and imidic acid tautomer called lactim. Both the tautomeric forms exist predominantly at neutral pH with the lactam structure being the most stable form [2].

Uracil molecule physisorption on the B40 fullerene surface with a binding distance of 2.38Å is investigated using non-equilibrium Green's function and density functional theory [3]. C-doped porous carbon nitrides prepared from uracil mediated molecule with cyanuric acid showed effective electron hole separation and broaden the light absorption range [4]. The uracil complexes of several metal ions, such as Fe(III), Co(III), Ni(II), Cu(II), Zn(II), Cd(II), and Pd(II) have been

*Corresponding author. E-mail: moamen@tu.edu.sa ; msrefat@yahoo.com

This work is licensed under the Creative Commons Attribution 4.0 International License

reported earlier [5-13]. Literature review reveals that uracil behaves as monobasic bidentate ligand bonding through $N_{(1)}$ and $C_{(4)}=O$ [8]. A number of monomeric metal complexes of uracil have been reported in the literature in which the chelation of uracil occurs either through $N_{(3)}$ and $C_{(2)}=O$, or through $N_{(3)}$ and $C_{(4)}=O$ [9, 10]. However, the polymeric mixed ligand complexes of uracil or substituted uracil generally involve $N_{(1)}$ and $C_{(4)}=O$ in bonding with metal ion [11-13]. The uracil-metal complexes can have square planar and octahedral geometries [3, 4]. Uracil's substituted in position five stand out in bioactivity, with various biological activities including antiviral properties, anticancer, cytotoxic, anti-mycobacterial, and antitumor, to antibacterial [14-23]. In this manuscript we aim to synthesize new Mg(II), Ca(II), Sr(II) and Ba(II) complexes of uracil and report an assessment of their coordination behavior using spectral measurements and thermal studies. In view of the continuous interest of antimicrobial agents we deemed it worthwhile to investigate the antimicrobial activity of Mg(II), Ca(II), Sr(II) and Ba(II) uracil complexes to assess their antimicrobial potential.

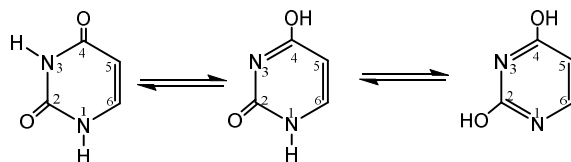


Figure 1. Tautomeric forms of uracil.

EXPERIMENTAL

Chemicals

In this work, the purity of the used chemicals was very high and did not require any additional purification. Sigma-Aldrich Chemical Company, USA provided uracil, $MgCl_2 \cdot 6H_2O$, $CaCl_2$, $SrCl_2 \cdot 6H_2O$ and $BaCl_2 \cdot 2H_2O$ chemical compounds.

Measurements

The elemental analyses of carbon, hydrogen and nitrogen contents were performed by the microanalysis unit at Cairo University, Egypt, using a Perkin Elmer CHN 2400 (USA). The molar conductivity using Jenway 4010 conductivity meter was measured regarding the freshly prepared uracil complex dissolved in dimethyl sulfoxide solvent with concentration 10^3 M. The infrared spectra were recorded on a Bruker FT-IR Spectrophotometer ($4000-400$ cm^{-1}). 1H -NMR measurements were performed on a Bruker DRX-250 spectrometer. Samples were dissolved in dimethyl sulfoxide- d_6 with TMS as internal reference. The thermal studies TG-50H were carried out on a Shimadzu thermogravimetric analyzer under static air till 800 $^{\circ}C$. Scanning electron microscopy (SEM) images were taken in Quanta FEG 250 equipment.

Anti-bacterial activities experiment.

Disc diffusion technique was used to evaluate the antibacterial activity of synthesized compounds against test bacteria strains based on measurement of disc inhibition clear zone (mm). Kanamycin and Ampicillin were used as positive reference standard drugs against positive-gram and negative-gram testes strains respectively.

Method of synthesis

Uracil (2 mmol, 0.1120 g) in each case was dissolved in methanol/H₂O (20 mL) and the whole was heated to reflux at 75 °C for 30 min. To this solution, 1 mmol each of MgCl₂ (0.0952 g), CaCl₂ (0.1109 g) SrCl₂ (0.1585) or BaCl₂ (0.2082 g) in hot ethanol (10 mL) was added and the mixture was heated to reflux for 3 h, resulting in a clear solution. From this solution, the metal complexes were precipitated by raising the pH to 5–6 by adding dropwise 0.2 M sodium hydroxide. The fine precipitates were heated on a water bath for ca. 15 min to increase their particle size. They were then filtered off, washed with ethanol and diethyl ether successively and dried in an oven at 50 °C. The physical and chemical properties of the synthesized metal complexes were confirmed as follows:

[Mg(C₄H₄N₂O₂)₂(H₂O)₂]Cl₂. Color: white; m. p. > 300 °C; Yield: 80%; ¹H NMR (DMSO-d₆ and CDCl₃ mixture, 600 MHz): δ = 2.94 (s, 4H, 2H₂O), 5.22 (d, 4H, J = 7.8 Hz, C₅-H), 7.14 (d, 4H, J = 7.8 Hz, C₆-H), 10.62 (s, 2H, N₁-H), 10.69 (s, 2H, N₂-H). ¹³C NMR (DMSO-d₆ and CDCl₃ mixture, 150 MHz): δ = 100.44 (C₅), 143.26 (C₅), 151.95 (C₂=O), 163.49 (C₄=O). Anal. calcd. for C₈H₁₂Cl₂MgN₄O₆ (355.41): C, 27.04; H, 3.40; Cl, 19.95; N, 15.76; found C, 26.87; H, 3.31; Cl, 19.78; N, 15.71; Λ_m = 69 S cm² mol⁻¹.

[Ca(C₄H₄N₂O₂)₂(H₂O)₂]Cl₂. Color: white; m. p. > 300 °C; Yield: 76%; ¹H NMR (DMSO-d₆ and CDCl₃ mixture, 600 MHz): δ = 3.01 (s, 4H, 2H₂O), 5.51 (d, 4H, J = 7.8 Hz, C₅-H), 7.14 (d, 4H, J = 7.8 Hz, C₆-H), 10.71 (s, 2H, N₁-H), 10.81 (s, 2H, N₂-H). ¹³C NMR (DMSO-d₆ and CDCl₃ mixture, 150 MHz): δ = 101.11 (C₅), 142.45 (C₅), 151.43 (C₂=O), 162.85 (C₄=O). Anal. calcd. for C₈H₁₂CaCl₂N₄O₆ (371.18): C, 25.89; H, 3.26; Cl, 19.10; N, 15.09; found C, 25.73; H, 3.15; Cl, 18.86; N, 14.78; Λ_m = 63 S cm² mol⁻¹.

[Sr(C₄H₄N₂O₂)₂(H₂O)₂]Cl₂. Color: white; m. p. > 300 °C; Yield: 73%; ¹H NMR (DMSO-d₆ and CDCl₃ mixture, 600 MHz): δ = 3.08 (s, 4H, 2H₂O), 5.49 (d, 4H, J = 9.0 Hz, C₅-H), 7.15 (d, 4H, J = 7.8 Hz, C₆-H), 10.72 (s, 2H, N₁-H), 10.82 (s, 2H, N₂-H). ¹³C NMR (DMSO-d₆ and CDCl₃ mixture, 150 MHz): δ = 101.22 (C₅), 142.51 (C₅), 151.42 (C₂=O), 162.88 (C₄=O). Anal. calcd. for C₈H₁₂Cl₂N₄O₆Sr (418.73): C, 22.95; H, 2.89; Cl, 16.93; N, 13.38; found C, 22.85; H, 2.80; Cl, 16.82; N, 13.24; Λ_m = 66 S cm² mol⁻¹.

[Ba(C₄H₄N₂O₂)₂(H₂O)₂]Cl₂. Color: white; m. p. > 300 °C; Yield: 79%; ¹H NMR (DMSO-d₆ and CDCl₃ mixture, 600 MHz): δ = 3.00 (s, 4H, 2H₂O), 5.51 (d, 4H, J = 7.8 Hz, C₅-H), 7.14 (d, 4H, J = 7.8 Hz, C₆-H), 10.71 (s, 2H, N₁-H), 10.81 (s, 2H, N₂-H). ¹³C NMR (DMSO-d₆ and CDCl₃ mixture, 150 MHz): δ = 101.18 (C₅), 142.44 (C₅), 151.45 (C₂=O), 162.89 (C₄=O). Anal. calcd. for C₈H₁₂BaCl₂N₄O₆ (468.43): C, 20.51; H, 2.58; Cl, 15.14; N, 11.96; found C, 20.27; H, 2.41; Cl, 14.98; N, 11.77; Λ_m = 71 S cm² mol⁻¹.

RESULTS AND DISCUSSION*Elemental and conductance data*

The new synthesized chelates of Mg(II), Ca(II), Sr(II) and Ba(II) with uracil was prepared by adding equimolar amounts of salts MgCl₂, CaCl₂, SrCl₂ and BaCl₂ to uracil. The structures of the ligand and the complexes were established from their IR, ¹H-NMR spectra, elemental analyses, and magnetic susceptibility measurements. The complexes are intensely colored stable solids, and the high molar conductance value for the complexes Mg(II), Ca(II), Sr(II) and Ba(II) are 69, 63, 66 and 71 ohm⁻¹ cm² mol⁻¹, respectively, at ambient temperature indicating electrolytic in nature. It is clearly from the conductance data that these complexes have an ionic nature, and they are of

the electrolyte type. Interestingly, the conductance measurements of the resulted complexes confirm the proposed general formulae as suggested that two chloride ions outside the coordination sphere depending upon elemental analyses. The results of the elemental analysis (Table 1) of the uracil and its metals complexes are in good agreement with those calculated for the suggested formula and agree with a 1:2 metal to ligand stoichiometry for all the complexes.

Table 1. Elemental analysis and physico-analytical data for uracil and its metal complexes.

Complexes M.Wt./ (M.F.)	Yield%	m.p./°C	Color	Found (calcd.), %				Λ_m ($\Omega^{-1} \cdot \text{cm}^2 \cdot \text{mol}^{-1}$)
				C	H	N	Cl	
$\text{C}_4\text{H}_4\text{N}_2\text{O}_2$ (Ura) 112.09	--	> 300	white	42.86 (42.86)	3.60 (3.60)	24.99 (24.99)	--	17.94
$[\text{Mg}(\text{Ura})_2(\text{H}_2\text{O})_2]\text{Cl}_2$ 335.41/ ($\text{C}_8\text{H}_{12}\text{Cl}_2\text{MgN}_4\text{O}_6$)	80	> 300	white	27.04 (26.87)	3.40 (3.31)	15.76 (15.71)	19.95 (19.78)	69.0
$[\text{Ca}(\text{Ura})_2(\text{H}_2\text{O})_2]\text{Cl}_2$ 371.18/ ($\text{C}_8\text{H}_{12}\text{CaCl}_2\text{N}_4\text{O}_6$)	76	> 300	white	25.89 (25.73)	3.23 (3.15)	15.09 (14.78)	19.10 (18.86)	63.0
$[\text{Sr}(\text{Ura})_2(\text{H}_2\text{O})_2]\text{Cl}_2$ 418.73/ ($\text{C}_8\text{H}_{12}\text{Cl}_2\text{N}_4\text{O}_6\text{Sr}$)	73	> 300	white	22.95 (22.85)	2.89 (2.80)	13.38 (13.24)	16.93 (16.82)	66.0
$[\text{Ba}(\text{Ura})_2(\text{H}_2\text{O})_2]\text{Cl}_2$ 468.43/ ($\text{C}_8\text{H}_{12}\text{BaCl}_2\text{N}_4\text{O}_6$)	79	> 300	white	20.51 (20.27)	2.58 (2.41)	11.96 (11.77)	15.14 (14.98)	71.0

The presence of chloride ions as hydrated ions reported by qualitative reaction is in good agreement with molar conductivity data. The thermal nature of the complexes has been obtained by TGA analysis. The formation of uracil complexes frameworks and bidentate ON donor nature of the uracil with metal ions for the formation of complexes were obtained from characteristic band positions in FTIR and ^1H NMR, thermal and elemental analysis. These data of the metal complexes suggest that metal to ligand ratio of the metal complexes 1:2 stoichiometry of the types of $[\text{M}(\text{Ura})_2(\text{H}_2\text{O})_2]\text{Cl}_2$ where M is Mg(II), Ca(II), Sr(II) or Ba(II) as shown in Figure 2.

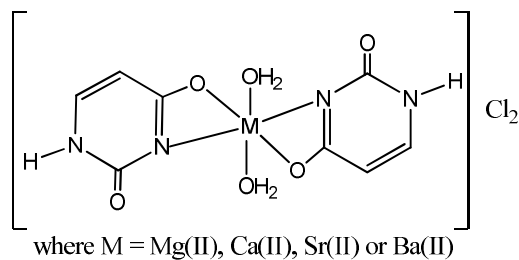


Figure 2. The structures of the coordination complexes.

Infrared spectra of uracil complexes.

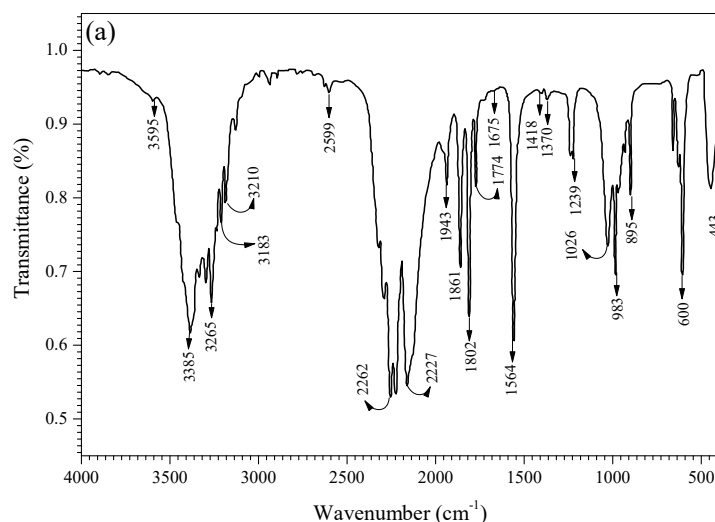
Important IR frequencies of uracil and its complexes are given in Table 2 while their spectra are shown in Figure 3. Several absorption bands in the 3000–3400 cm^{-1} region may be attributed to -NH and -OH stretching modes. The $\nu(\text{O-H})$ band at 3086, 3092, 3094 and 3091 cm^{-1} in the magnesium(II), calcium(II), Strontium(II) and barium(II) complexes, respectively, indicate the presence of water or the OH group. The infrared spectrum of the free ligand shows a strong broad band at 1675 cm^{-1} characteristic of ($\text{C}_{(4)}=\text{O}$) and a shoulder at 1774 cm^{-1} corresponding to ($\text{C}_{(2)}=\text{O}$), which are practically overlapped. Two weak/medium bands are observed at 3335 and 3265 cm^{-1} , which may be assigned to ($\text{N}_{(3)}\text{-H}$) and ($\text{N}_{(1)}\text{-H}$) stretching vibrations, respectively. The $\nu(\text{C}=\text{O})$

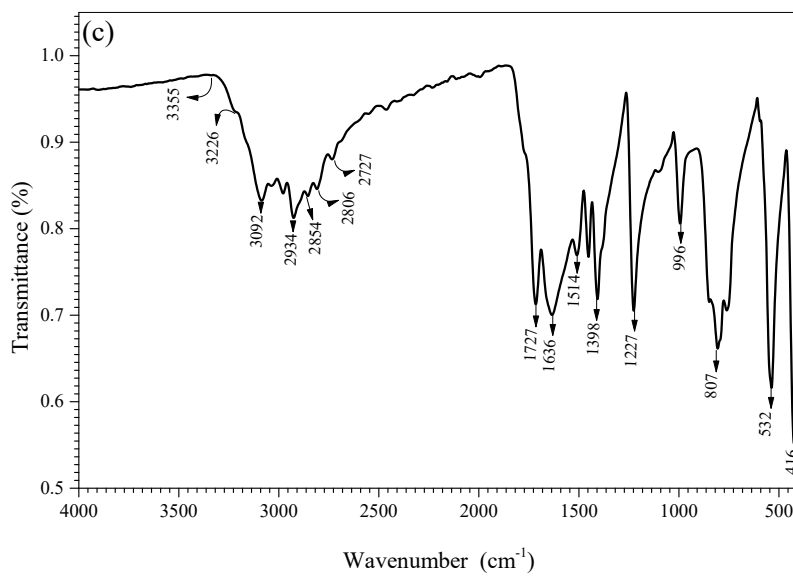
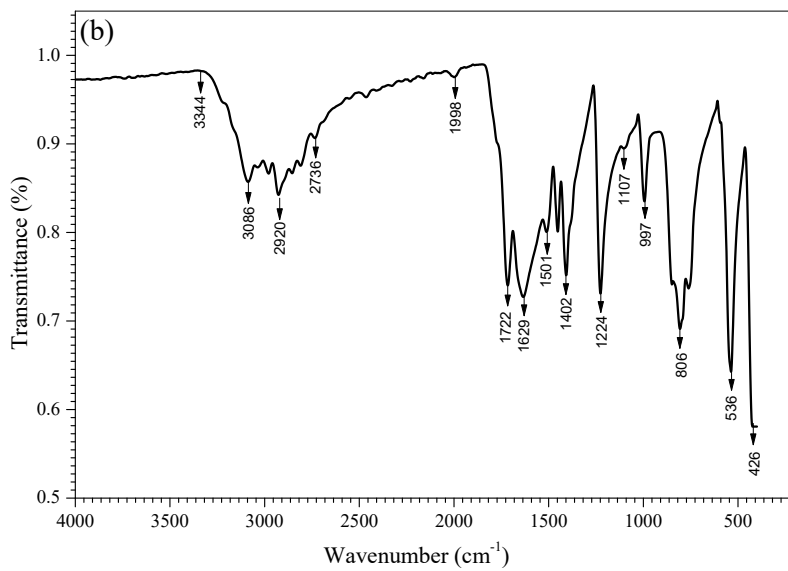
of the free ligand is observed at 1675 cm^{-1} , while the corresponding vibrations in the metal complexes are observed in the range of $1629\text{-}1645\text{ cm}^{-1}$. A shift of $30\text{-}45\text{ cm}^{-1}$ to lower frequencies is observed for the carbonyl band after coordination with the metal ions, clearly indicating the coordination of the carbonyl group to the metal ions. The disappearance of the absorption band at 3335 cm^{-1} ($\text{N}_{(3)}\text{-H}$ in the complex spectra indicates that the $\text{N}_{(3)}$ atom is bound to the metal ions. The complex spectra show an absorption band in the range of $1629\text{-}1645\text{ cm}^{-1}$. This band is not observed in the spectrum of the free ligand and may be attributed to the stretching motion associated with the $\text{C}=\text{N}$ bond resulting from the transformation of the ligand from the keto form to the enol form upon complexation.

Table 2. Important IR spectral data of uracil complexes.

Assignments	Uracil	Mg(II)	Ca(II)	Sr(II)	Ba(II)
$\nu(\text{OH}), \text{H}_2\text{O}$	--	3086	3092	3094	3359
$\nu(\text{N}_{(1)}-\text{H})$	3265	2920	2934	2930	2920
$\delta(\text{N}_{(3)}-\text{H})$	1418	1402	1398	1411	1417
$\nu(\text{C}-\text{H}), \text{aromatic}$	3210	2736	2854	2854	2851
$\nu(\text{C}_{(2)}=\text{O})$	1774	1722	1727	1723	2731
$\nu(\text{C}_{(4)}=\text{O})$	1675	1629	1639	1635	1645
$\nu(\text{C}=\text{N})$	1564	1501	1514	1505	1455
$\nu(\text{C}-\text{N}), \nu(\text{C}-\text{O})$	1239	1224	1227	1217	1224
$\nu(\text{M}-\text{O})$	--	536	532	540	535
$\nu(\text{M}-\text{O})$	--	426	416	422	416

The observation of such a band in the complex spectra support the assumption that uracil is coordinated with the metal ions as a bidentate ligand through one oxygen atom of the carbonyl group and the $\text{N}_{(3)}$ atom. This coordination mode is also supported by the observation of two weak bands in the ranges of $540\text{-}532$ and $416\text{-}426\text{ cm}^{-1}$, which are attributed to $\text{M}-\text{N}$ and $\text{M}-\text{O}$ stretching modes, respectively. These two bands are not observed in the spectrum of the free ligand [24-28]. According to the forgoing discussion and based on the proposed molecular formulas, the probable structures of the $\text{Mg}(\text{II})$, $\text{Ca}(\text{II})$, $\text{Sr}(\text{II})$, and $\text{Ba}(\text{II})$ complexes are in octahedral geometries as shown in Figure 2 [29-31].





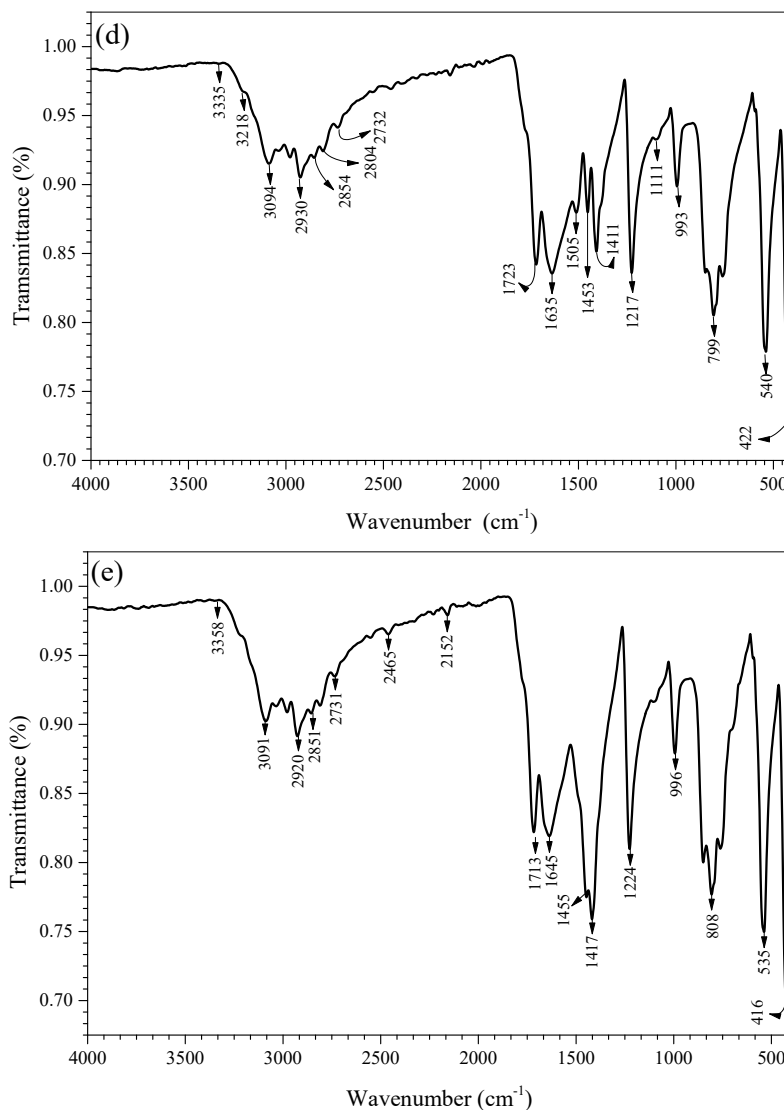


Figure 3. FTIR spectrum of uracil free ligand (a), Mg(II) (b), Ca(II) (c), Sr(II) (d) and Ba(II) (e) complexes.

Thermal decomposition studies (TGA)

The results of thermogravimetric analyses of uracil and its complexes are given in Table 3. The thermograms were performed in the range of 30–700 °C at a heating rate of 10 °C/min in nitrogen atmosphere. They displayed an agreement in weight loss between their consequences achieved from the thermal decomposition and the considered values, supporting the results of elemental analysis, and confirming the proposed formulae as shown in Figure 2. The free ligand completely

decomposes in one step at approximately 320 °C, indicating its pure organic structure. The thermal decomposition for $[\text{Mg}(\text{C}_4\text{H}_4\text{N}_2\text{O}_2)_2(\text{H}_2\text{O})_2]\text{Cl}_2$ complex exhibits three degradation steps as shown in Fig. 4b. The Mg(II) complex loss upon heating two coordinated water molecules in the first stage at maximum temperature 100 °C is accompanied by weight loss (7.98%). The second step of decomposition occurs at maxima temperature 300 °C is accompanied by weight loss (28.92%) corresponding to the loss of $\text{Cl}_2 + \text{HCN}$. The third step of decomposition occurs at maxima temperature of 500 °C and is accompanied by a weight loss (49.91%) corresponding to the loss of $2\text{NCOH} + \text{CO} + \text{C}_2\text{H}_2 + \text{HNCH}$ then the final thermal decomposition product obtained is MgO. $[\text{Ca}(\text{C}_4\text{H}_4\text{N}_2\text{O}_2)_2(\text{H}_2\text{O})_2]\text{Cl}_2$ was stable up to 80 °C and its decomposition started at 80 °C and finally completed at 800 °C. The TG temperatures of 80–260 °C, 260–500 °C, 500–800 °C, caused by loss of H_2O molecule, Cl^- , NCOH and breakdown of the uracil ligand molecule, the remaining mass seems likely to correspond to CaO. The overall estimated weight loss amounts to 81.07 % (calc. 80.00%). TGA curve of $[\text{Sr}(\text{C}_4\text{H}_4\text{N}_2\text{O}_2)_2(\text{H}_2\text{O})_2]\text{Cl}_2$ complex shows no weight loss up to 50 °C. Thereafter, it loses two water molecules between 50 and 200 °C indicating that these are coordinated water. The second step of decomposition occurs at in the temperature range 200–300 °C is accompanied by weight loss (31.05%) corresponding to the loss of $\text{Cl}_2 + 2\text{NO}$. Lastly, the remaining bonded hydrazide ligand is removed from the complex in the range 300–495 °C then the final thermal decomposition product obtained is $\text{SrO} + 0.5\text{C}$. The decomposition reactions of $[\text{Ba}(\text{C}_4\text{H}_4\text{N}_2\text{O}_2)_2(\text{H}_2\text{O})_2]\text{Cl}_2$ occur in three step from 50 °C to 800 °C. In this complex, the first decomposition step proceeds at a temperature between 50 °C and 200 °C with a weight loss ranging from of 7.69%, associated with the loss of the two coordinated water content. The second step of decomposition occurs at in the temperature range 200–400 °C is accompanied by weight loss (27.79 %) corresponding to the loss of $\text{Cl}_2 + \text{NO}$. The third step of decomposition occurs at in the temperature range 400–800 °C and is accompanied by a weight loss (37.97%) corresponding to the loss of $\text{C}_2\text{H}_2 + \text{NO} + 2\text{HNCH} + \text{CO} + \text{H}_2 + \text{O}_2$ then the final thermal decomposition product obtained is $\text{BaO} + 0.5\text{C}$.

Table 3. Thermal decomposition of the uracil ligand and their metal complexes.

Compound	Steps	Temp. range (°C)	Weight loss (%)		Lost species
			Obs.	Cal	
$\text{C}_4\text{H}_4\text{N}_2\text{O}_2$ (Ura) 112.09	One step	350	99.6	100	$\text{C}_4\text{H}_4\text{N}_2\text{O}_2$
$\text{C}_8\text{H}_{12}\text{Cl}_2\text{MgN}_4\text{O}_6$ 335.41	1 st step 2 nd step 3 rd step Residue	100 – 300 300 – 500 500 – 800	7.98 28.92 49.91 12.02	7.91 28.16 49.84 11.98	$2\text{H}_2\text{O}$ $\text{Cl}_2 + \text{HCN}$ $2\text{NCOH} + \text{CO} + \text{C}_2\text{H}_2 + \text{HNCH}$ MgO
$\text{C}_8\text{H}_{12}\text{CaCl}_2\text{N}_4\text{O}_6$ 371.18	1 st step 2 nd step 3 rd step Residue	80 – 260 260 – 500 500 – 800	9.70 30.44 40.93 18.33	9.68 30.51 40.81 18.42	$2\text{H}_2\text{O}$ $\text{Cl}_2 + \text{NCOH}$ $\text{C}_2\text{H}_2 + \text{HCN} + \text{NCOH} + \text{HNCH}$ + CO CaO + C
$\text{C}_8\text{H}_{12}\text{Cl}_2\text{N}_4\text{O}_6\text{Sr}$ 418.73	1 st step 2 nd step 3 rd step Residue	50 – 200 200 – 300 300 – 800	8.6 31.05 34.4 25.45	8.67 31.11 34.35 25.36	$2\text{H}_2\text{O}$ $\text{Cl}_2 + 2\text{NO}$ $\text{C}_2\text{H}_2 + 2\text{HNCH} + \text{CO} + \text{H}_2 + \text{O}_2$ $\text{SrO} + 0.5\text{C}$
$\text{C}_8\text{H}_{12}\text{BaCl}_2\text{N}_4\text{O}_6$ 468.43	1 st step 2 nd step 3 rd step Residue	50 – 200 200 – 400 400 – 800	7.69 27.79 30.74 33.37	7.73 27.75 31.00 33.42	$2\text{H}_2\text{O}$ $\text{Cl}_2 + \text{NO}$ $\text{C}_2\text{H}_2 + \text{NO} + 2\text{HNCH} + \text{CO} + \text{H}_2$ + O_2 $\text{BaO} + 0.5\text{C}$

The kinetic studies

The kinetic and thermodynamic parameters; the energy of activation (E), the pre-exponential factor (Z), the enthalpy of activation (ΔH^*), the entropy of activation (ΔS^*) and the Gibbs energy change (ΔG^*), together with the correlation coefficient (r) for the non-isothermal decomposition of the metal complexes, were determined by the Coats–Redfern integral method [32] and the Horowitz–Metzger (HM) approximation method [33]. The entropy, (ΔS^*), enthalpy, (ΔH^*) and the free energy change of activation, (ΔG^*), were evaluated using the following equations:

$$\Delta S^* = 2.303[\log(Ah/KT)]R \quad (1)$$

$$\Delta S^* = E^* - RT \quad (2)$$

$$\Delta G^* = \Delta H^* - T\Delta S^* \quad (3)$$

The evaluated kinetic parameters for the metal complexes based on the Coats–Redfern and Horowitz–Metzger equations are listed in Table 4. The activation energy of the complexes is expected to increase with increasing thermal stability of complexes. Hence, the E^* values for $C_8H_{12}Cl_2MgN_4O_6$ and $C_8H_{12}Cl_2N_4O_6Sr$ complexes are much higher than the other complexes, which indicate the higher thermal stability of $C_8H_{12}Cl_2MgN_4O_6$ and $C_8H_{12}Cl_2N_4O_6Sr$ complexes. The complexes show negative entropy values which indicate that the complexes under study have more ordered structures than the reactants and the reaction rates are slower than normal.

Table 4. Kinetic parameters determined using the Coats–Redfern (CR) and Horowitz–Metzger (HM).

Compound	Method	Parameter					r
		E^* (J. mol ⁻¹)	A $\times 10^3$ (s ⁻¹)	$\Delta S^* \times 10^2$ (J. mol ⁻¹ K ⁻¹)	ΔH^* $\times 10^4$ (J. mol ⁻¹)	ΔG^* $\times 10^4$ (J. mol ⁻¹)	
$C_8H_{12}Cl_2MgN_4O_6$	CR	2.87×10^5	6.18	-0.1883	28.4	27.7	0.9987
	HM	1.93×10^5	0.90	-0.2076	2.40	1.63	0.9968
$C_8H_{12}CaCl_2N_4O_6$	CR	3.43×10^3	6.41	-0.1874	0.11	0.55	0.9975
	HM	0.12×10^3	0.78	-0.1875	19.0	18.3	0.9962
$C_8H_{12}Cl_2N_4O_6Sr$	CR	3.08×10^4	7.56	-0.1849	2.81	2.21	0.9975
	HM	23.6×10^4	0.29	-0.2172	0.02	0.22	0.9895
$C_8H_{12}BaCl_2N_4O_6$	CR	2.47×10^3	6.63	-0.1862	0.02	0.58	0.9956
	HM	9.68×10^3	0.56	-0.2109	0.069	0.018	0.9816

¹H NMR spectra

The ¹H NMR spectral data uracil and its metal complexes in DMSO are summarized in Table 5. The spectra reveal a characteristic signal for the aromatic proton in its expected region of 7.00–8.00 ppm. The N(1)–H signal is located at 11.02 ppm in the spectrum of the free ligand, while the corresponding signals in the spectra of the Mg(II), Ca(II), Sr(II) and Ba(II) complexes are observed at 10.62, 10.71, 10.72, 10.71 and 10.82 ppm, respectively. The N(3)–H signal in the free ligand spectrum (11.52 ppm) is absent in the spectra of the complexes, which is consistent with the suggestion that uracil reacted with the metal ions through its enol form. The ¹H NMR spectra of Mg(II), Ca(II), Sr(II) and Ba(II) complexes in DMSO-*d*₆ exhibit the O–H proton signal at δ : 2.94 ppm, 3.01 ppm and 3.08 ppm and 3.00 ppm, due to the presence of water molecules in the complexes. On comparing main signals of uracil with its complexes, it was observed that all the signals of the free uracil were present in the spectra of the complexes with chemical shift upon binding with Mg(II), Ca(II), Sr(II) and Ba(II).

Table 5. ^1H NMR chemical shifts (ppm) for uracil and its metal complexes.

Assignments	S, 4H, 2H ₂ O	C5 – H	C6 – H	N1 – H	N2 – H
Uracil	--	5.47	7.40	10.82	11.02
C ₈ H ₁₂ Cl ₂ MgN ₄ O ₆	2.94	5.22	7.14	10.62	10.69
C ₈ H ₁₂ CaCl ₂ N ₄ O ₆	3.01	5.51	7.14	10.71	10.81
C ₈ H ₁₂ Cl ₂ N ₄ O ₆ Sr	3.08	5.49	7.15	10.72	10.82
C ₈ H ₁₂ BaCl ₂ N ₄ O ₆	3.00	5.51	7.14	10.71	10.81

SEM and TEM investigations

To study the surface morphology of our synthesized complexes, Mg(II), Ca(II), Sr(II) and Ba(II), transmission electron microscopy (TEM) and scanning electron microscopy (SEM) were utilized. The SEM micrograph of Mg(II) displays flattered morphology with small sized grains scattered on solid matrix and gives the appearance of river base like structure. The SEM of Ca(II) complex indicated tubular rods like morphology. The micrographs of Sr(II) complex indicated that the presence of well-defined crystals free from any shadow of the metal ion on their external surface had a twisted fiber and grass like morphology. The SEM micrograph of Ba(II) complex displays agglomerated morphology with small sized grains scattered in homogenous matrix and gives the appearance of coral-like structure. Images of TEM for [Mg(Ura)₂(H₂O)₂]Cl₂, [Ca(Ura)₂(H₂O)₂]Cl₂, [Sr(Ura)₂(H₂O)₂]Cl₂ and [Ba(Ura)₂(H₂O)₂]Cl₂ complexes are shown in Figure 4 and refer to the formation of spherical black spots with particle sizes starting from a few nanometers to several hundred.

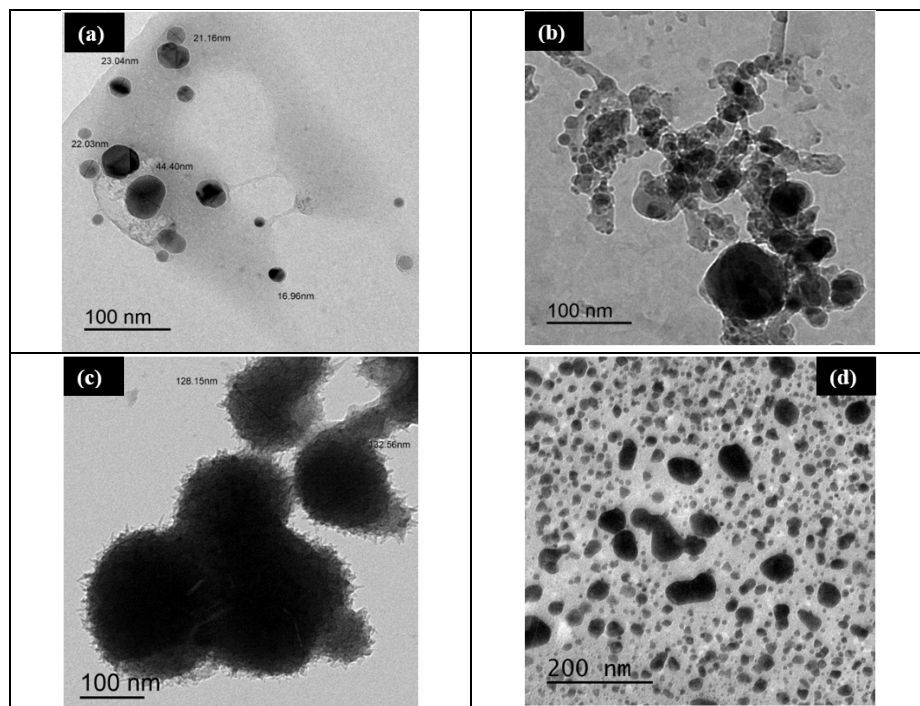


Figure 4. TEM images of (a) Mg(II), (b) Ca(II), (c) Sr(II) and (d) Ba(II), complexes.

Biological evaluation

For uracil complexity, the antibacterial activities against Gram-positive bacteria (*S. aureus*) and Gram-negative bacteria (*E. coli*) are presented in Table 6. The inhibition zone diameters (in mm) for the Ampicillin against gram-positive bacteria (*S. aureus*) and gram-negative bacteria (*E. coli*) give 15.66 and 0 mm, respectively, but the Kanamycin drug against (*S. aureus*) and (*E. coli*) gave 0 and 12, respectively. The *in vitro* antibacterial activities of the synthesized uracil complexes under investigation were tested against two bacterial strains, i.e. Gram-positive bacteria (*S. aureus*) and Gram-negative bacteria (*E. coli*). Compound $C_8H_{12}CaCl_2N_4O_6$, $C_8H_{12}Cl_2N_4O_6Sr$, $C_8H_{12}BaCl_2N_4O_6$ are the most active substance among the tested samples against the following gram-positive bacteria *E. coli*. Compound $C_8H_{12}CaCl_2N_4O_6$ (2) was the most active substance among the tested samples against the following gram-positive bacteria *S. aureus* (7 mm) and was more potent than the reference drug. Moreover, its antibacterial activity was significant against gram-negative bacteria *E. coli*, with an inhibition zone of 6 mm comparing to the other compounds. The synthesized compounds $C_8H_{12}Cl_2MgN_4O_6$ showed no activity against Gram-positive bacteria (*S. aureus*) and Gram-negative bacteria (*E. coli*), and the antibacterial activity seemed to be dependent on the nature of basic skeleton of the molecules [34,35].

Table 6. Antibacterial activities for the uracil and its complexes.

Compounds	Inhibition zone (mm) ^a antibacterial activity (1 mg/mL)	
	Gram-positive	Gram-negative
	<i>Staphylococcus aureus</i>	<i>Escherichia coli</i>
Control: DMSO	0	0
Ampicillin	15.66	0
Kanamycin	0	12
uracil	0	0
$C_8H_{12}Cl_2MgN_4O_6$	0	0
$C_8H_{12}CaCl_2N_4O_6$	7	6
$C_8H_{12}Cl_2N_4O_6Sr$	6	0
$C_8H_{12}BaCl_2N_4O_6$	6	6

^aThe values (average of triplicate) are diameter of zone of inhibition at 1 mg/mL.

CONCLUSION

Four new Mg(II), Ca(II), Sr(II), and Ba(II) complexes with uracil ligand were synthesized and characterized by physicochemical and spectroscopic techniques. In all the complexes uracil is coordinated with the metal ions as a bidentate ligand through one oxygen atom of the carbonyl group and the N₍₃₎ atom. The presence of coordinated or non-coordinated water in metal complexes was confirmed by thermal and IR data. The TGA curves of all the compounds were similar in character and the parameters such as E^* , ΔS^* , ΔH^* , and ΔG^* were calculated. The complexes were screened for their antibacterial activities, and $C_8H_{12}CaCl_2N_4O_6$, $C_8H_{12}Cl_2N_4O_6Sr$, $C_8H_{12}BaCl_2N_4O_6$ complexes exhibited antimicrobial activities against various bacterial compared with standard drugs.

ACKNOWLEDGMENTS

The researchers would like to acknowledge Deanship of Scientific Research, Taif University for funding this work.

REFERENCES

1. Pauer, A.W.; Tadeusz, M.K.; Halina, S. Intramolecular interactions in derivatives of uracil tautomers. *Molecules* **2022**, *27*, 7240.
2. Deepthi, R.; Balaji, G.V.; Tharanikkarasu K. Therapeutic potential of uracil and its derivatives in countering pathogenic and physiological disorders. *Eur. J. Med. Chem.* **2022**, *207*, 112801.
3. Kaur, J.; Kumar, R.; Vohra, R.; Sawhney, R.S. Density functional theory investigations on the interaction of uracil with borospherene. *Bull. Mater. Sci.* **2022**, *45*, 22.
4. Wen, J.; Wang, Y.; Zhao, H.; Zhang, M.; Zhang, S.; Liu, Zhai, Y. Uracil-mediated supramolecular assembly for C-enriched porous carbon nitrides with enhanced photocatalytic hydrogen evolution. *New J. Chem.* **2022**, *46*, 4647-4653.
5. Krishan, K.N.; Vinod, P.S.; Bhattacharya, D. Synthesis, characterization and antitumour activity of uracil and uracil-histidine complexes with metal(III). *Trans. Metal. Chem.* **1997**, *22*, 333-337.
6. Hossein, T. Study of binding energies using DFT methods, vibrational frequencies and solvent effects in the interaction of silver ions with uracil tautomers. *Arabian J. Chem.* **2017**, *10*, S786-S799.
7. Wang, M.S.; Rong, J.W.; Ke-Chen, L.Q.; Wei, Y.Q. Theoretical studies on the binding of Cd²⁺ to uracil and its thio-derivatives. *Chin. J. Struct. Chem.* **2012**, *31*, 521-527.
8. Vinod, P.S.; Karishma, T.; Monika, M. Synthesis, spectral and thermal studies of some polymeric mixed ligand uracil-hydrazide complexes with transition metal ions. *Des. Monomers Polym.* **2013**, *16*, 456-464.
9. Ghosh, P.; Mukhopadhyaya, T.; Sarkar, A. Interaction of divalent metal-ions with uracil complexes of Mn(II), Fe(II), Co(II), Ni(II) and Cu(II) with uracil acting as bidentate ligand. *Trans. Met. Chem.* **1984**, *9*, 46-48.
10. Ali, O.Y.; Fridgen, T.D. Structures of electrosprayed Pb(Uracil-H) (+) complexes by infrared multiple photon dissociation spectroscopy. *Int. J. Mass Spectrom.* **2011**, *308*, 167-174
11. Singh, V.P.; Singh, A. 5-Bromouracil and 5-bromouracil-histidine complexes with metal(II) ions and their antitumour activity. *Trans. Met. Chem.* **2004**, *29*, 107-111.
12. Singh, V.P.; Singh, S.; Narang, K.K.; Bhattacharya, D. Aluminium(III), chromium(III) and iron(III) complexes with 5-iodouracil and 5-iodouracil-histidine and their antitumour activity. *J. Enz. Inh. Med. Chem.* **2009**, *24*, 105-110.
13. Narang, K.K.; Singh, V.P.; Bhattacharya, D. Synthesis, characterization and antitumour activity of uracil and uracil-histidine complexes with metal(III) ions. *Trans. Met. Chem.* **1997**, *22*, 333-337.
14. Mohammed, B.A.; Ashraf, A.A.; Bahaa, G.M.; Youssif, S.B.; Akil, A.B. B.; Mahmoud, A.A.; Asmaa, H.M. Design and synthesis of new thiazolidinone/uracil derivatives as antiproliferative agents targeting EGFR and/or BRAF^{V600E}. *Front Chem.* **2022**, *10*, 1076383.
15. Shatha, M.H.O. Synthesis, characterization and antibacterial activities of uracil and uracil-oxalate complexes with Cr(III) and Fe(III). *Eng. Technol. J.* **2019**, *37*, 6-16
16. Mohammed, M.Y.; Abdul Karim, M.G.; Abdel Karim, H.M. Synthesis, characterization, and bacterial activity of Co(II), Ni(II), and Pd(II) complexes with ligands of thymine, uracil thiuram disulfur, and cyclic amines. *Macromol. Symp.* **2022**, *401*, 2100310.
17. Nishithendu, B.N.; Atanu, P.; Julia, K.; Rakesh, G.; Susanta, G.; Tarun, K.M. Copper(II) complexes of 1,3-dimethyl-5-(4/3'-pyridylazo)-6-aminouracil: Structures, redox, magnetic and protein binding properties. *J. Mol. Struct.* **2022**, *15*, 132164.
18. Tanase, C.I.; Draghici, C.; Cojocaru, A.; Galochkina, A.V.; Orshanskaya, J.R.; Zarubaev, V.V.; Shova, S.; Enache, C.; Maganu, M. New carbocyclic N6-substituted adenine and pyrimidine nucleoside analogues with a bicycle [2.2.1] heptane fragment as sugar moiety; synthesis, antiviral, anticancer activity and X-ray crystallography. *Bioorg. Med. Chem.* **2015**, *23*, 6346-6354.

19. Gimadieva, A.R.; Khazimullina, Y.Z.; Belaya, E.A.; Zimin, Y.S.; Abdrakhmanov, L. B.; Mustafin, A.G. Express evaluation of antioxidant activity of uracil derivatives. *Biomed. Khim.* **2015**, *61*, 765-769.
20. Palasz, A.; Ciez, D. In search of uracil derivatives as bioactive agents. Uracils and fused uracils: Synthesis, biological activity and applications. *Eur. J. Med. Chem.* **2015**, *97*, 582-611.
21. Tanase, C.I.; Draghici, C.; Cojocaru, A.; Galochkina, A.V.; Orshanskaya, J.R.; Zarubaev, V.V. New carbocyclic N6-substituted adenine and pyrimidine nucleoside analogues with a bicyclo[2.2.1]heptane fragment as sugar moiety; synthesis, antiviral, anticancer activity and X-ray crystallography. *Bioorg. Med. Chem.* **2015**, *23*, 6346-6354.
22. Isobe, Y.; Tobe, M.; Inoue, Y.; Isobe, M.; Tsuchiya, M.; Hayashi, H. Structure and activity relationships of novel uracil derivatives as topical antiinflammatory agents. *Bioorg. Med. Chem.* **2003**, *11*, 4933-4940.
23. Seferoglu, Z.; Ertan, N. Synthesis, characterization and spectroscopic properties of some new phenylazo-6-aminouracil. *Open Chem.* **2008**, *6*, 81-88.
24. Bertrand, B.; Nisole, C.; Drancourt, J.M.; Dubuffet, T.; Bouchet, J.P.; Volland, J.P. Determination of cis and trans configurations in pentahydrobenzopyranopyrroles by FT-IR spectroscopy. *Spectrochim. Acta Part A* **1996**, *52*, 1921-1923.
25. Suffren, Y.; Rollet, F.; Reber, C. Raman spectroscopy of transition metal complexes: molecular vibrational frequencies, phase transitions, isomers, and electronic structure. *Comments Inorg. Chem.* **2011**, *32*, 246-276.
26. Nakamoto, K. *Infrared and Raman Spectra of Inorganic and Coordination Compounds*, 6th ed., John Wiley and Sons Inc.: Canada; **2009**.
27. Günzler, H.; Germlich, H. *IR Spectroscopy: An Introduction*, Wiely-VCH Verlag: Weinheim (Germany); **2002**.
28. Mostafa, S.I.; Kabil, M.A.; Saad, E.M.; El-Asmy, A.A. Ligational and analytical applications of a uracil derivative toward some transition metal ions. *J. Coord. Chem.* **2006**, *59*, 279-293.
29. Sarkar, A.R.; Ghosh, P. Interaction of divalent metal ions with uracil. I. Oxygen coordinating uracil complexes of Mn(II), Fe(II), Co(II), Ni(II) and Cu(II). *Inorg. Chim. Acta* **1983**, *78*, 39-41.
30. Kufelnicki, A.; Jaszczak, J.; Kalinowska-Lis, U.; Wardak, C.; Ochocki, J. Complexes of uracil (2,4-dihydropyrimidine) derivatives. *J. Solution Chem.* **2006**, *35*, 739-751.
31. Gaballa, A.S.; Teleb, S.M.; Asker, M.S.; Yalçin, E.; Seferoğlu, Z. Synthesis, spectroscopic properties and antimicrobial activity of some new 5-phenylazo-6-aminouracil-vanadyl complexes. *J. Coord. Chem.* **2011**, *64*, 4225-4243.
32. Coats, A.W.; Redfern, J.P. Kinetic parameters from thermogravimetric data. *Nature* **1964**, *201*, 68-69.
33. Horowitz, H.W.; Metzger, G.A. A new analysis of thermogravimetric traces. *Anal. Chem.* **1963**, *35*, 1464-1668.
34. El-Bindary, M.A.; El-Bindary, A.A. Synthesis, characterization, DNA binding, and biological action of dimedone arylhydrazone chelates. *Appl. Organomet. Chem.* **2022**, *36*, e6576.
35. El-Bindary, M.A.; El-Desouky, M.G.; El-Bindary, A.A. Metal-organic frameworks encapsulated with an anticancer compound as drug delivery system: Synthesis, characterization, antioxidant, anticancer, antibacterial, and molecular docking investigation. *Appl. Organomet. Chem.* **2022**, *36*, e6660.